

Studies on ejector-venturi fume scrubber

Sudip Kumar Das^{a,*}, Manindra Nath Biswas^b

^a Chemical Engineering Department, University of Calcutta, 92 A.P.C. Road, Kolkata 700 009, India

^b Chemical Engineering Department, Indian Institute of Technology, Kharagpur 721 302, India

Received 5 November 2005; received in revised form 15 March 2006; accepted 17 March 2006

Abstract

Experimental studies on diesel fume scrubbing have been conducted in a down-flow type liquid-jet ejector-venturi scrubber. The fume particulates have been captured in the throat of the ejector-venturi by a mechanism involving inertial impaction and impingement. The effect of nozzle geometry and the motive fluid flow rates on the suction created and the volumetric fume aspiration rates have been analyzed, in order to select the optimum nozzle geometry. Using the optimum nozzle geometry the efficiency of fume collection has been experimentally investigated as function of various hydrodynamic parameters. A theoretical analysis has been performed to interpret the experimental findings and determination of nozzle loss coefficients.

© 2006 Elsevier B.V. All rights reserved.

Keywords: Ejector; Venturi; Scrubber; Fume

1. Introduction

The objectionable fumes discharged from various process industries are rarely composed of a single component. In general the fume exhausts are composed of solid or liquid aerosols, vapors and gases, and are characterized by the presence of aerosols of less than 0.1 μm in size. The bad odors that are associated with the fumes exhausts are chiefly due to vaporous constituents and liquid aerosols, rather than solid particulates. Fumes have detrimental effect on plants, human beings and other living creatures. The severity and nature of effect depend upon the individual characteristics of the components. Based on their sources fume generation may be classified into the following categories: (i) fumes generated from automobiles and household activities; (ii) fumes generated from various metallurgical processes; (iii) fumes generated in manufacturing industries; (v) fumes from the ceramic industries; (vi) fumes evolved from the effluents of chemical process industries. If the diameter of the aerosol is less than 0.1 μm , they may be collected by the mechanism of Brownian diffusion and when it is much above 0.1 μm the mechanism of impaction becomes important.

Several options are available for the control of particulate matter such as cyclones, fabric filters, electrostatic precipitators

and various types of wet scrubbers. Amongst the wet scrubbers, the venturi scrubber is very efficient for the collection of particulates and it can also be used as gas absorber. Consequently, venturi scrubbers find application wherever; simultaneous control of particulates and gaseous species is needed. They are also employed for the control of aerosols, fumes and odors from gas streams. Some of the main advantages of venturi scrubbers are high particulate collection efficiencies, simple in design, low initial cost of equipment, and ability to handle large volumes of gases in relatively small-sized equipment. One disadvantage is the high-pressure drop of the gas side [1]. Ejector-venturi scrubbers are versatile tools for a large amount of applications related to gaseous pollutants removal. Since there are no moving parts within the scrubber, it is ideal for handling for many situations, particularly sticky or abrasive materials.

An ejector is a device in which the kinetic energy of a motive (primary) fluid is utilized for suction, mixing and dispersion of a secondary fluid and when used as a device for gas-liquid contacting the secondary fluid may be dispersed by the shearing action of the high velocity motive fluid or the motive fluid itself may get dispersed when it is arrested by a secondary fluid. Efficient functioning of an ejector depends on the design of the suction chamber, the mixing throat, the divergent diffuser and the forcing nozzle. Besides, the relative dimensions of the various parts of the ejector, the factors such as shape of the entrance to the parallel throat, angle of divergence and the projection ratio defined as the ratio of the distance between the nozzle tip

* Corresponding author. Tel.: +91 33 2566 7650; fax: +91 33 2351 9755.
E-mail address: sudipcuce@hotmail.com (S.K. Das).

Nomenclature

a_d	diffuser cross-sectional area (m ²)
a_t	throat cross-sectional area (m ²)
A	jet cross-sectional area (m ²)
A_d	area ratio of the diffuser outlet to the throat
A_n	area of the nozzle (m ²)
A_r	area ratio of the throat to the nozzle
d_n	diameter of the nozzle (m)
d_t	diameter of the throat (m)
F_g	gravitational force (kg m/s ²)
g	acceleration due to gravity (m/s ²)
L_d	length of the diffuser (m)
L_t	length of the throat (m)
N_t	number of transfer unit
p_0, p_t, p	pressure at respective section (Pa)
ΔP_d	pressure loss in the diffuser (N/m ²)
P_T	contacting power (W/m ³ /s)
ΔP_{th}	pressure loss in the throat (N/m ²)
Q_l	liquid flow rate (m ³ /s)
Q_g	gas flow rate (m ³ /s)
S_d	loss coefficient in the diffuser
S_{th}	loss coefficient in the throat

Greek letters

α	characteristic parameter in Eq. (26)
β	characteristic parameter in Eq. (26)
η	collection efficiency
ρ	density (kg/m ³)
τ	shear stress (N/m ²)

Subscripts

g	gas
l	liquid
0, t, d	to the position as in Fig. 2
w	wall

and the throat entry to the throat diameter, are also important. Two types of ejector throat shapes have been reported in the literature, namely, the constant area mixing type (with cylindrical mixing throat) and the constant pressure mixing type (with convergent–divergent mixing throat). Furthermore, it has been reported that the constant area mixing type ejector gives a better performance than the constant pressure mixing type [2–4].

The high-energy dissipation rates in the ejector throat result in the formation of very small bubble diameters and consequently into the generation of very high interfacial area [5]. This gives better gas–liquid mass transfer rates and higher rates of reaction. Thus ejectors have been used for gas sparging in bubble columns. Many researchers [6–12] used the momentum and mass balance equations across the ejector to obtain the rate of gas entrainment. Different researchers [5,11–15] have also carried out the experimental investigation on the effects of different operating parameters on the ejector performance. From the review of the literature it can be observed that ejectors and similar devices are being increasingly used for gas–liquid dispersion, mixing,

mass and heat transfer operations, etc. because of the simple construction containing no moving parts, good sealing performance, capability of handling flammable or explosive gases, meeting erosive or radiative conditions, large interfacial area generation and intense mixing between the phases. In addition such devices can be used to carry out chemical reactions as they combine the functions of flow inducing devices and mixing reactors.

In co-current down-flow column, bubbles are forced to move in a direction opposite to their buoyancy, the residence time of the gas is more and also the contact efficiency is higher when compared to an up flow bubble column. If the pressure at the top of the column is lower than the atmospheric pressure, the spontaneous injection of gas is possible. In the down-flow bubble column, the liquid velocity must be higher than the bubble rise velocity and under this condition the coalescence of bubbles are minimized. If the liquid velocity is low enough, the downward flow of the large bubbles is suppressed and the gas gradually accumulates at the top of the column. As a result, stable operation becomes impossible. Therefore, the range of stable operation of the down-flow bubble column is quite narrow [12,16–18]. The two-phase vertical down-flow system has few advantages, i.e., bubbles are finer and more uniform in size, bubbles coalescence is negligible, gas–liquid contact is more and the flow structure is homogeneous in nature [19].

This paper deals with an experimental study on the performance of a downward oriented liquid-jet ejector-venturi scrubber and investigates its applicability as a fume exhaust-scrubber. Since the performance of the system is expected to depend very strongly on the type, size and number of the nozzles exhaustive investigations have been carried out on the maximum suction created and the aspiration rates at various suction conditions, for various nozzle sizes. Theoretical compatibility of the experimental data has also been investigated.

2. Theoretical consideration

The following assumptions are made for the development of the fluid flow equations:

1. The two-phases (gas and liquid) flow coaxially in the throat and diffuser section.
2. The heat generated effect due to the shear between the individual molecules and between the molecules and the wall are negligible.
3. No mass transfer takes place between the two-phases.
4. There is no phase change, i.e., condensation or evaporation.
5. The flow stream is one dimensional at throat entry and exit.
6. The presence of liquid-jet expansion between nozzle outlet and the mixing point in the contactor is neglected.

2.1. Analysis for the evaluation of loss coefficient in the throat

The momentum balance equation in the throat is as follows:

$$(p_0 - p_t)a_t + \tau_w a_w + F_g = (m_l v_{lt} + m_g v_{gt}) - (m_l v_{l0} + m_g v_{g0}) \quad (1)$$

As there is no mixing in the throat, momentum transfer between the phases can be neglected, so the above Eq. (1) reduced to,

$$(p_0 - p_t)a_t + \tau_w a_w + F_g = 0 \quad (2)$$

Shear stress can be defined by the following expression:

$$\frac{4\tau_w L_t}{d_t} = \frac{S_{th}\rho_1 v_{in}^2}{2} \quad (3)$$

$$\tau_w a_w = \left(\frac{S_{th}\rho_1 v_{in}^2}{2} \right) a_t \quad (4)$$

The gravitational force can be expressed as

$$F_g = a_t L_t g (\rho_l + \rho_g) \quad (5)$$

As, $\rho_l \gg \rho_g$ the above Eq. (5) reduced to

$$F_g = a_t L_t g \rho_l \quad (6)$$

Putting $\tau_w a_w$ from Eq. (4) and F_g from Eq. (6) into Eq. (2) we get,

$$(p_0 - p_t)a_t - \left(\frac{S_{th}\rho_1 v_{in}^2}{2} \right) a_t + a_t L_t g \rho_l = 0 \quad (7)$$

or,

$$\Delta P_{th} - \frac{S_{th}\rho_1 v_{in}^2}{2} + L_t g \rho_l = 0 \quad (8)$$

or,

$$S_{th} = \frac{2(\Delta P_{th} + L_t g \rho_l)}{\rho_1 v_{in}^2} \quad (9)$$

or,

$$S_{th} = \frac{2A_n^2(\Delta P_{th} + L_t g \rho_l)}{Q_1^2 \rho_1} \quad (10)$$

2.2. Analysis for the evaluation of loss coefficient in the diffuser

An energy balance equation in the differential form for the gas–liquid flow in the diffuser section can be presented as

$$\frac{dp}{\rho_{lt}} + V dV + d \frac{\Delta P_d}{\rho_{lt}} - g dz = 0 \quad (11)$$

As $\rho_{lt} = \rho_l$, we may write

$$\frac{dp}{\rho_l} + V dV + d \frac{\Delta P_d}{\rho_l} - g dz = 0 \quad (12)$$

where

$$\Delta P_d = S_d \frac{\rho_l V_{in}^2}{2} \quad (13)$$

Putting Eq. (13) into Eq. (12), we get

$$\frac{dp}{\rho_l} + V dV + S_d d \frac{V_{in}^2}{2} - g dz = 0 \quad (14)$$

Integration between ‘t’ and ‘d’ and subsequent rearrangement gives

$$(p_d - p_t) + \rho_l \left(V_{1d}^2 - \frac{V_{1t}^2}{2} \right) - \rho_l g L_d + S_d \left(\frac{V_{1n}^2}{2} \right) = 0 \quad (15)$$

Now V_{1t} and V_{1d} can be expressed by the following notations:

$$V_{1t} = \frac{Q_{1t}}{a_t} = \frac{V_{in}}{A_r} \quad (16)$$

$$V_{1d} = \frac{Q_{1d}}{a_d} = V_{1d} \left(\frac{A_d}{A_r} \right) \quad (17)$$

and subsequent substitution in Eq. (15) gives

$$(p_d - p_t) + \rho_l \left(\frac{V_{in}^2 A_d^2 - V_{1n}^2}{2A_r^2} \right) - \rho_l g L_d + S_d \left(\frac{V_{1n}^2}{2} \right) = 0 \quad (18)$$

or,

$$\frac{\Delta P_d}{\rho_l} + V_{in}^2 \left(\frac{A_d^2 - 1}{2A_r^2} \right) - g L_d + \frac{1}{\rho_l} S_d \left(\frac{V_{1n}^2}{2} \right) = 0 \quad (19)$$

or,

$$S_d = \frac{2}{\rho_l V_{1n}^2} (\Delta P_d + g L_d) - \frac{A_d^2 - 1}{A_r^2} \quad (20)$$

or,

$$S_d = \frac{2A_n^2}{\rho_l Q_1^2} (\Delta P_d + \rho_l g L_d) - \frac{A_d^2 - 1}{A_r^2} \quad (21)$$

2.3. Evaluation to calculate total fractional loss in ejector

The total loss (S) is taken as summation of throat and diffuser frictional losses.

2.4. Particulate collection

The conventional basis for expressing the degree of collection is the efficiency, η . The efficiency is generally an exponential function of the process variables for most types of collection equipment. Hence, a more fundamental basis for expressing the effectiveness of the ejector-venturi collection is the number of transfer units, N_t , and defined as

$$N_t = \ln \left(\frac{1}{1 - \eta} \right) \quad (22)$$

or,

$$\eta = 1 - e^{-N_t} \quad (23)$$

The contact power theory relates particulate collection efficiency in scrubber to the pressure drop for the gas phase plus any power expanded in atomizing the liquid. In venturi scrubber, however, one can neglect the pressure drop due to gas flow,

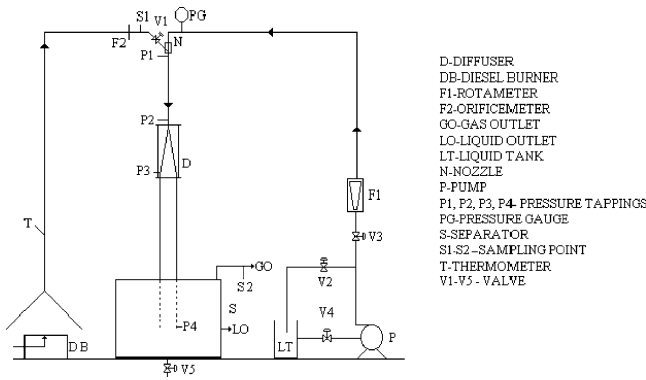


Fig. 1. Schematic diagram of experimental setup.

Table 1
Ejector dimension

Throat diameter (mm)	19.05
Throat length (mm)	148.00
Diffuser angle (°)	8.6
Diffuser length (mm)	210
Diffuser outlet diameter (mm)	50.08
Secondary fluid inlet diameter (mm)	10.05

which is insignificant to the power required for expanding in atomizing the liquid. So,

$$P_1 = 150 p_1 \left(\frac{Q_l}{Q_g} \right) \quad (24)$$

and

$$P_T = P_1 \quad (25)$$

For a given scrubber and particulate properties a very distinct relationship has been established between number of transfer unit and the contacting power,

$$N_t = \alpha P_T^\beta \quad (26)$$

where α and β are the characteristic parameters.

3. Experimental

The experimental setup shown in Fig. 1 consists of three parts, namely the ejector assembly, the liquid introduction side and gas introduction side. A constant area mixing type of liquid-jet ejector has been used for the experiments. Fig. 2 shows the schematic diagram of the ejector-venturi scrubber system. The dimension of ejector is shown in Table 1. The ejector assembly consists of five parts:

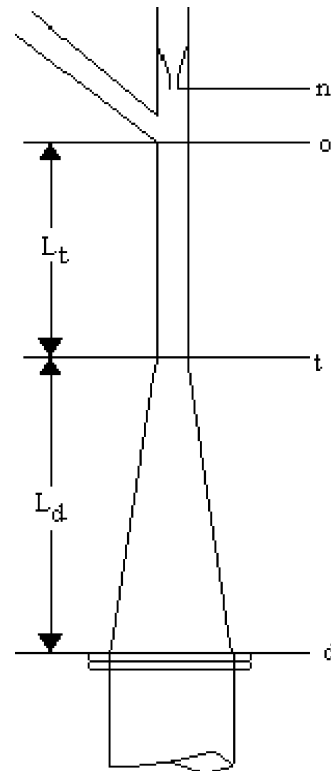


Fig. 2. Schematic diagram of ejector-venturi scrubber related to momentum balance.

- (i) The motive fluid is introduced through nozzles. Three types of nozzles have been used for the present investigation and their specification is shown in Table 2.
- (ii) The aspirated gas enters through a suction chamber, whose volume in the present case was kept minimized and the gas enters through a contoured entrance without any shock or mixing losses. The liquid and the gas inlet are met at an angle of 62°. Both inlet nozzles have been encased in a solid Perspex block.
- (iii) The throat is made of a smooth Perspex tube of 0.024 m in outside diameter and 0.125 m in length. The upper and the lower portion of the throat was threaded and inserted into the suction chamber and the diffuser section, respectively.
- (iv) The diffuser section is a diverging nozzle, whose upstream edge has the same dimension as throat and the downstream edge has an inside diameter of 5.16 cm. The length of the diffuser is 0.204 m. It is made of Perspex and the angle of the divergence of the diffuser is 7°.
- (v) The straight section is originating from the diffuser outlet and inserted well into the separator vessel. The length and

Table 2
Nozzle specification

Type	Number of orifice	Diameter of each orifice (cm)	Triangular pitch centre to centre distance (cm)	Flow area (cm ²)	Area ratio
1	1	0.66	–	0.3422	0.0644
2	3	0.28	0.45	0.1818	0.0342
3	5	0.16	0.30	0.0989	0.0168

Table 3

Position of the pressure tapings along the vertical axis of the ejector-venturi scrubber

Nomenclature of the tapings	Distance from the throat entrance (m)
p1	0.04
p2	0.24
p3	0.48
p4	1.14

outside diameter of the straight pipe, made of Perspex, is 2.5 m and 5.16 cm, respectively.

- (vi) The separator vessel is a Perspex cylindrical chamber of 0.45 m in height and 0.31 m in diameter. The straight pipe has been inserted into vessel and its lower edge is 20 cm above the floor level. It has been provided with a Perspex gas outlet of 5.0 cm diameter. A sample taping, S2, was provided to collect the particulate at the gas outlet. The separator was also provided with a drain line fitted with a gate valve.
- (vii) The liquid introduction side helps to maintain a constant supply of liquid into ejector-venturi system during experimental run. This section consists of a liquid storage tank, a centrifugal pump, and valves for control the flow rate, rotameters, pressure gages, etc.
- (viii) In the gas introduction section the fume was generated by burning diesel and was fed to the gas inlet of the ejector. A globe valve, V1, controlled the flow rate of the aspirated gas. The gas introduction line was a Perspex line of 5.0 cm diameter. This line was provided with an orifice meter and thermometer to measure the flow and temperature of the secondary fluid. A sampling point, S1, has been installed at a distance of 5.0 cm from the gas inlet nozzle.
- (ix) Static pressure is measured in the different points of the test section and their positions are shown in Table 3.

In the first part of the study, hydrodynamics of the system has been investigated with a view to determine the loss coefficient, maximum suction created for a particular nozzle and liquid rate, gas–liquid flow ratio obtainable at different suction pressure. Water as motive and air as secondary fluids were used with three different nozzles. To determine the maximum suction created the motive fluid was sprayed through the nozzle keeping the secondary fluid inlet closed. A single-phase flow, with the liquid-jet completely submerged with the liquid continuum resulted and the manometer connected in the suction line showed the vacuum created. Now the secondary fluid inlet was opened in steps, thereby permitting the secondary fluid to flow into the suction chamber. The secondary fluid mixed intensively with the motive fluid in the throat, the divergent nozzle and in the extended contactor. As the valve in the suction line opens more and more gradually, increase in secondary flow resulted and mixing between gas and liquid was intensified still for a particular position of the inlet valve, where the flow is separated out. At the point of separation jet flow was observed in the system with negligible secondary flow. Values of motive fluid rate, maximum suction created, secondary fluid rate at various suction pressures have been noted for individual nozzle.

Table 4

Ranges of operating variables used during experimentation system: air–water

Types of nozzle	Liquid flow rate ($\times 10^3 \text{ m}^3/\text{s}$)	Liquid inlet pressure (kPa)	Air flow rate ($\times 10^6 \text{ m}^3/\text{s}$)
1	0.233–0.5	143.25–244.5	10.116–364.16
2	0.233–0.35	279.5–356.4	21.12–170.175
3	0.166–0.233	279.5–454.2	15.698–211.93

Table 5

Ranges of operating variables investigated system: diesel exhaust fume–water

Nozzle used	Type 2
Liquid flow rate	0.183×10^{-3} to $0.35 \times 10^{-3} \text{ m}^3/\text{s}$
Liquid inlet pressure	248.5–356.4 kPa
Fume rate	46.3×10^{-6} to $792.8 \times 10^{-6} \text{ m}^3/\text{s}$
Particulate concentration of inlet fumes	172.2–158.78 mg/m^3
Temperature of inlet fume	76–86 °C
Rate of sampling	0.8–1.4 LPM

In the second part of the experiment, the secondary fluid is air contaminated with controlled quantities of diesel fumes. The concentration of particulates was measured by drawing out known volume of gas sample by water displacement meter through glass-fibre filters and amount of particle deposited was determined gravimetrically.

The range of operating variables used during the experimentation is shown in Tables 4 and 5.

4. Results and discussion

4.1. Operating regimes

The jet energy is being utilized in the air entrainment, gas–liquid mixing, and the two-phase down-flow. In general the different flow regimes, i.e., bubble flow, churn-turbulent flow and slug flow depend on the gas superficial velocity for a particular column diameter. The flow regime is primarily depends on the liquid flow rate. However, homogeneous bubbly flow is the most desirable as it gives maximum contact area but it depends

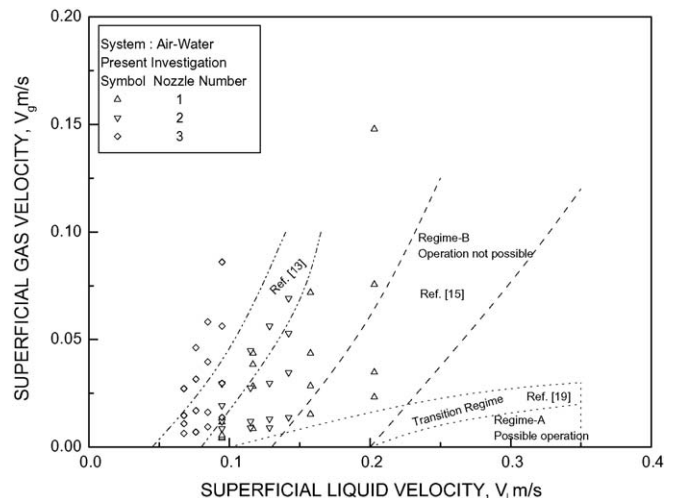


Fig. 3. Flow regime map of stable co-current down-flow.

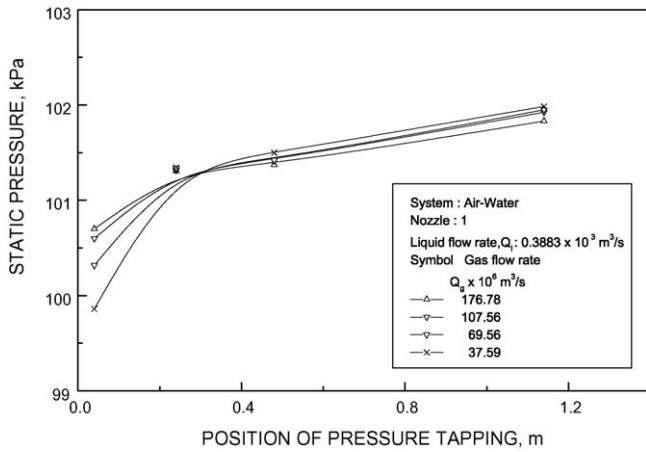


Fig. 4. Static pressure distribution along the ejector vertical axis at a fixed water flow rate for different gas flow rate and nozzle 1.

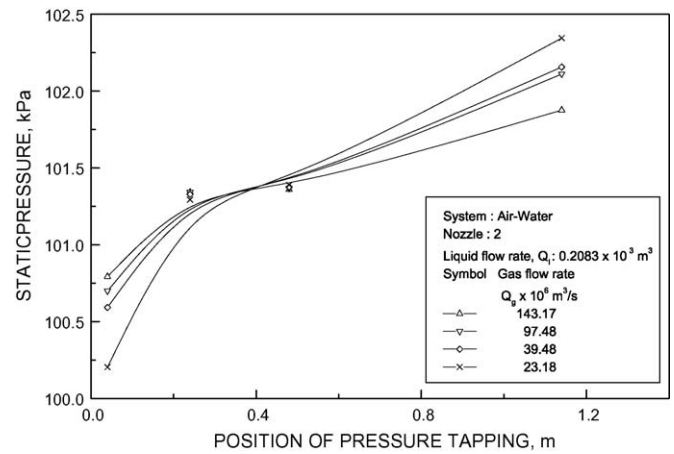


Fig. 6. Static pressure distribution along the ejector vertical axis at a fixed water flow rate for different gas flow rate and nozzle 3.

on the liquid-jet flow rate. As the liquid flow rate increases the gas bubbles coalesce to form large bubbles and heterogeneous churn-turbulent or slug flow results. Kulkarni and Shah [19] presented a flow regime map with a sparger type gas distributor and observed that (i) operating zone is only Regime-A, (ii) Regime-C is practically undesirable zone and (iii) Regime-B operation is not possible. Fig. 3 shows that the Regime-B is operating zone for the present studies and the range of operating variables are much wider in compared with other data [13,15,19]. Homogeneous bubbly flow is observed in the experimental condition.

4.2. Pressure profiles

Figs. 4–6 show some typical example of static pressure distribution along the vertical axis of the ejector-venturi scrubber for a particular nozzle at constant liquid flow rate with different gas flow rates. It is clear from the figures that the diffuser giving outlet pressure even higher than the pressure at the throat. This means that the system is capable of supplying a slight head of impulsion. Fig. 7 indicates that with increase in suction rate, the static pressure at the suction inlet decreases. The experimental result shows that the maximum pressure drop occurs

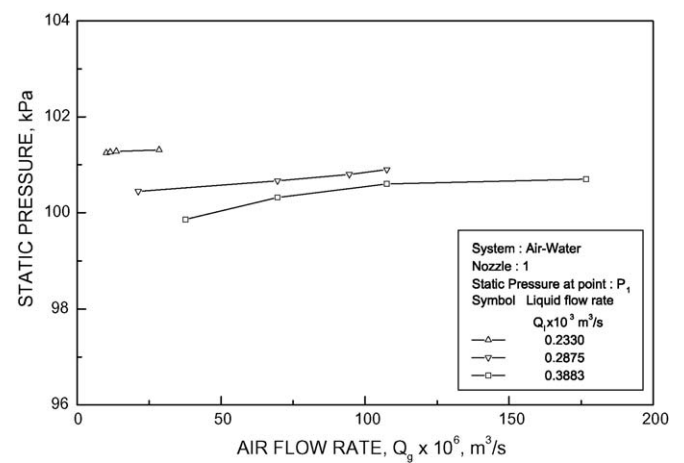


Fig. 7. Variation of static pressure at the throat with gas flow rate for different liquid flow rate.

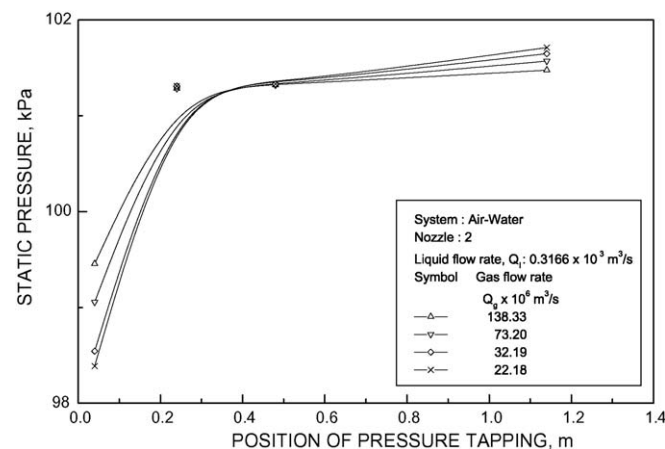


Fig. 5. Static pressure distribution along the ejector vertical axis at a fixed water flow rate for different gas flow rate and nozzle 2.

at the throat section. Atay et al. [20] also obtained the similar observation.

Fig. 8 shows the effect of the area ratio on the secondary fluid entrainment rate for constant motive fluid rate. With the increasing the area ratio the rate of entrainment is found to be decreasing

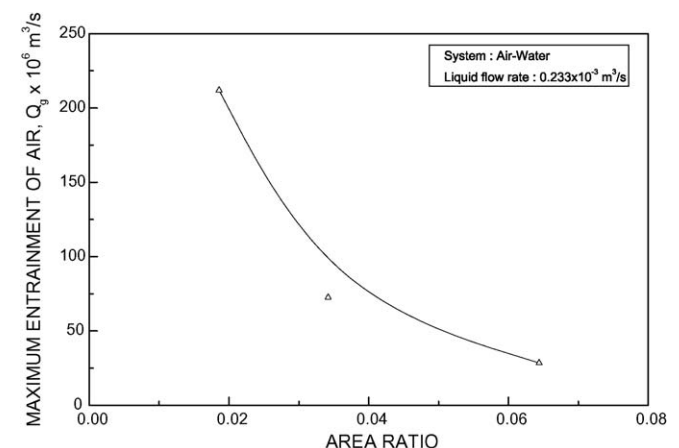


Fig. 8. Effect of area ratio for on the maximum air entrainment rate.

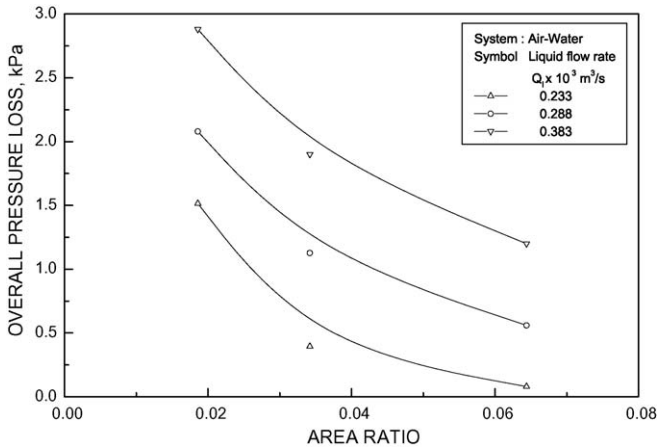


Fig. 9. Variation of area ratio on overall pressure drop at maximum suction rate.

as the effective liquid velocity decreases. Fig. 9 shows the variation of the area ratio on the overall pressure drop at maximum suction rate. It is clear from the figure that the overall pressure drop decreases with increasing the area ratio.

4.3. Loss coefficients

The various loss coefficients, namely the throat, the diffuser and the overall are plotted against the Reynolds number at the nozzle and are presented in Figs. 10–12. The graphical representation shows that the coefficient decreases as the Reynolds number increases. The diffuser and throat losses are to some extent interdependent. Longer the length of the throat, the flatter will be the velocity profile at the entry to the diffuser and less flow separation and pressure loss will occur. Conversely, attempts to reduce friction losses by the use of very short throat are likely to lead to very high losses in the diffuser unless very long slow tapers are used. There is, therefore, an optimum combination of throat length and diffuser taper. Since the maximum static pressure recovery takes place after about six to seven diameters of the throat and the velocity profile will be reasonably good, the following ranges of values reasonably appears to be good, $S_{th} = 0.15$ to 0.2 and $S_d = 0.15$ to 0.25 , depending on the taper [4].

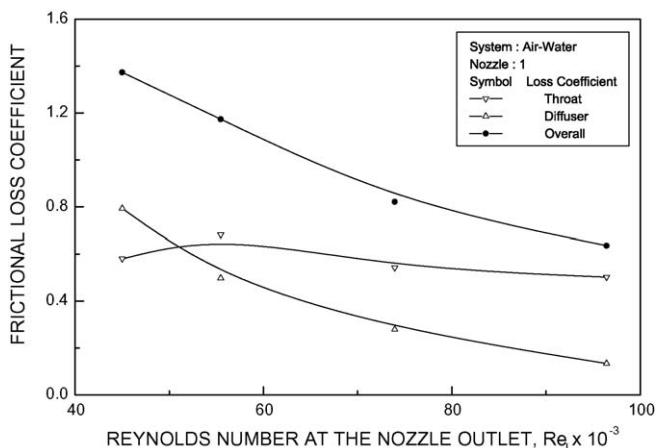


Fig. 10. Variation of loss coefficient against Reynolds number for nozzle 1.

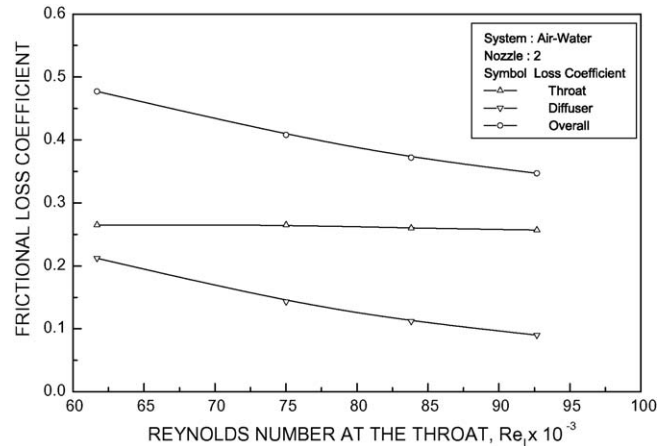


Fig. 11. Variation of loss coefficient against Reynolds number for nozzle 2.

Thus for designing purpose, a total loss, $S = 0.4$ will be reasonable and usually gives slightly pessimistic pressure efficiencies when compared with the experimental results [4].

The nozzle 2 is considered the best for the present investigation for fume particulate scrubbing because:

- The total frictional loss is in and around 0.4, which generally takes as the optimum design criteria,
- It can be used for a wider range of flow rate in compare to the nozzle 3,
- The visual observation indicates there is an improved mixing for nozzle 2 compared to nozzle 1.

4.4. Particulate scrubbing

Fig. 13 shows the removal efficiency of the fume increases exponentially with the water flow rate. Maximum removal efficiency is more than 97%.

Fig. 14 shows the variation of the number of transfer unit with the contact power. To quantify the amount of the particulate collection the contact power theory has been used and the result

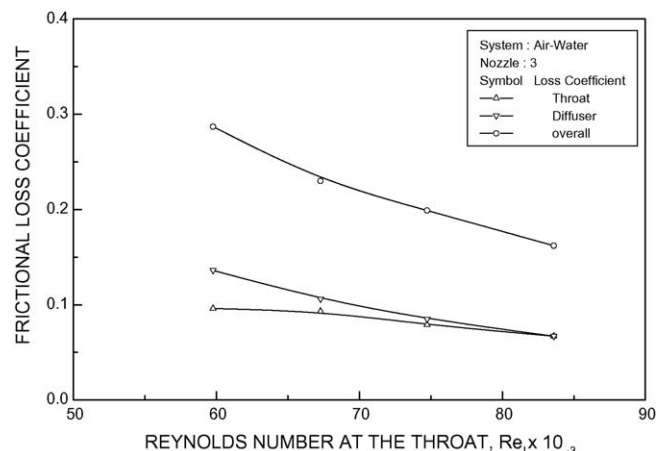


Fig. 12. Variation of loss coefficient against Reynolds number for nozzle 3.

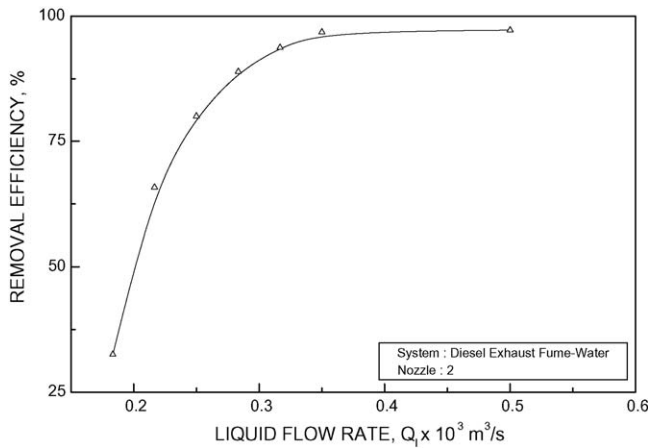


Fig. 13. Removal efficiency with the water flow rate.

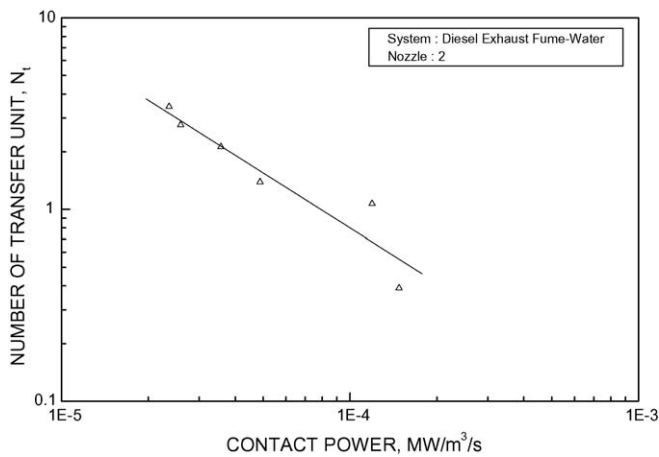


Fig. 14. Variation of NTU with the contact power.

is depicted as

$$N_t = 1.21 \times 10^{-4} P_T^{-0.95} \quad (27)$$

The equation indicates that with the increase in contact power the NTU decreases, i.e., the separation (or collection of the fumes) will be easier.

5. Conclusion

Experiments have been carried out in ejector-venturi scrubber for fume scrubbing. It has been found that the down-flow type of ejector-venturi scrubber can be conveniently used for fume scrubbing with out using any auxiliary gas moving equipment.

Nozzle loss coefficients were found out for both single nozzle and multi nozzle arrangements. The loss coefficients were determined using the theoretical equations using the experimental data. These results were used for the selection of the proper nozzle sizes for the fume scrubbing operation.

The optimized system was found to operate with much wider range of operating variables than those used by the other investigators [13,15,19]. The fume removal efficiency was found to be more than 97%.

In conclusion the ejector-venturi system can be used for the abatement of hazardous and toxic fumes in a convenient environment friendly manner.

References

- [1] M. Ravindram, N. Pyla, Modeling of a venturi scrubber for the control of gaseous pollutants, *Ind. Eng. Chem. Proc. Des. Dev.* 25 (1986) 35–40.
- [2] R.A. Smith, *Some Aspects of Fluid Flow*, Institute of Physics, Edward Arnold and Co., London, 1951, p. 229.
- [3] C.E. Lapple, *Fluid and Particle Mechanics*, University of Delaware, New York, UAS, 1956.
- [4] S.K. Chandraker, Gas dispersion in non-Newtonian liquid-jet ejectors and two-phase co-current vertical upflow, Ph.D. Thesis, Indian Institute of Technology, Kharagpur, India, 1985.
- [5] R.J. Malone, Loop reactor technology, improves catalytic hydrogenation, *Chem. Eng. Prog.* 78 (1980) 53–59.
- [6] G.S. Davies, A.K. Mitra, A.N. Roy, Momentum transfer studies in ejector, *Ind. Eng. Chem. Proc. Des. Dev.* 6 (1967) 293–299.
- [7] D.K. Acharjee, P.A. Bhat, A.K. Mitra, Studies on momentum transfer in vertical liquid jet ejectors, *Indian J. Chem. Technol.* 13 (1975) 205–210.
- [8] M.N. Biswas, A.K. Mitra, A.N. Roy, Effective interfacial area in a liquid-jet induced horizontal gas–liquid pipeline contactor, *Indian Chem. Eng.* 19 (2) (1977) 2–9.
- [9] D. Mukherjee, M.N. Biswas, A.K. Mitra, Hydrodynamics of liquid–liquid dispersion in ejectors and vertical two phase flow, *Can. J. Chem. Eng.* 66 (1988) 896–907.
- [10] J. Zahradnik, J. Kratochvil, F. Kastanek, M. Rylek, Energy effectiveness of bubble column reactors with sieve tray and ejector type gas distributors, *Chem. Eng. Commun.* 15 (1982) 27–40.
- [11] P. Havelka, V. Linek, J. Sinkule, J. Zahradnik, M. Fialova, Effect of the ejector configuration on the gas suction rate and the gas hold-up in ejector loop reactor, *Chem. Eng. Sci.* 52 (1997) 1701–1713.
- [12] G. Kundu, D. Mukherjee, A.K. Mitra, Experimental studies on a co-current gas–liquid downflow bubble column, *Int. J. Multiphase Flow* 21 (1995) 893–906.
- [13] M.N. Biswas, A.K. Mitra, Momentum transfer in horizontal multi-jet liquid-gas ejector, *Can. J. Chem. Eng.* 59 (1981) 634–637.
- [14] Y. Bando, M. Kuraishi, M. Hattori, T. Asada, Cocurrent down flow bubble column with simultaneous gas liquid injection-nozzle, *J. Chem. Eng. Jpn.* 21 (1988) 607–612.
- [15] A. Mandal, G. Kundu, D. Mukherjee, Gas holdup and entrainment characteristics in a modified downflow bubble column with Newtonian and non-Newtonian liquid, *Chem. Eng. Proc.* 42 (2003) 777–787.
- [16] P.C. Wright, V. Meeyoo, W.K. Soh, A study of ozone mass transfer in cocurrent downflow jet pump contactor, *Ozone Sci. Eng.* 20 (1997) 17–32.
- [17] X. Gamisans, M. Sarra, F.J. Lafuente, Fluid flow and pumping efficiency in an ejector-venturi scrubber, *Chem. Eng. Prog.* 43 (2004) 127–136.
- [18] A. Kulkarni, Y.T. Shah, Gas phase dispersion in a down flow bubble column, *Chem. Eng. Commun.* 28 (1984) 311–326.
- [19] I. Atay, G. Lewandowski, R. Trattner, Fluid flow and gas absorption in an ejector venturi scrubber, *Environ. Prog.* 6 (3) (1987) 198–203.